atmosphere

MDPI

Article

A Multimethod Analysis for Average Annual Precipitation Mapping in the Khorasan Razavi Province (Northeastern Iran)

Mehdi Aalijahan [1,2] and Azra Khosravichenar [3,4,*]

[1] Department of Physical Geography, Mohaghegh Ardabili University, Ardabil 5619911367, Iran; m.alijahan@uma.ac.ir
[2] Department of Physical Geography, University of Marmara, Istanbul 34722, Turkey
[3] Institute of Geography, Leipzig University, D-04103 Leipzig, Germany
[4] Department of Human Evolution, Max Planck Institute for Evolutionary Anthropology, D-04103 Leipzig, Germany
* Correspondence: azra_khosravichenar@eva.mpg.de or azra.khosravichenar@uni-leipzig.de; Tel.: +49-(0)-341-3550-764

Abstract: The spatial distribution of precipitation is one of the most important climatic variables used in geographic and environmental studies. However, when there is a lack of full coverage of meteorological stations, precipitation estimations are necessary to interpolate precipitation for larger areas. The purpose of this research was to find the best interpolation method for precipitation mapping in the partly densely populated Khorasan Razavi province of northeastern Iran. To achieve this, we compared five methods by applying average precipitation data from 97 rain gauge stations in that province for a period of 20 years (1994–2014): Inverse Distance Weighting, Radial Basis Functions (Completely Regularized Spline, Spline with Tension, Multiquadric, Inverse Multiquadric, Thin Plate Spline), Kriging (Simple, Ordinary, Universal), Co-Kriging (Simple, Ordinary, Universal) with an auxiliary elevation parameter, and non-linear Regression. Root Mean Square Error (RMSE), Mean Absolute Error (MAE), and the Coefficient of Determination (R^2) were used to determine the best-performing method of precipitation interpolation. Our study shows that Ordinary Co-Kriging with an auxiliary elevation parameter was the best method for determining the distribution of annual precipitation for this region, showing the highest coefficient of determination of 0.46% between estimated and observed values. Therefore, the application of this method of precipitation mapping would form a mandatory base for regional planning and policy making in the arid to semi-arid Khorasan Razavi province during the future.

Keywords: precipitation interpolation; distribution of precipitation; geostatistics; cross-validation; Khorasan Razavi province; northeastern Iran

Citation: Aalijahan, M.; Khosravichenar, A. A Multimethod Analysis for Average Annual Precipitation Mapping in the Khorasan Razavi Province (Northeastern Iran). *Atmosphere* **2021**, *12*, 592. https://doi.org/10.3390/atmos12050592

Academic Editor: Eduardo García-Ortega

Received: 20 March 2021
Accepted: 27 April 2021
Published: 2 May 2021

1. Introduction

Precipitation systems can be mainly regrouped in convective and stratiform events, and the main worldwide observed rainfall patterns can be considered as a combination of these two components [1]. Considering the tempo-spatial changes of precipitation on the one hand, and an often relatively low density of rain gauge stations on the other hand, it is common to estimate, rather than measure, the precipitation distribution over a larger area. The obtained isohyetal map describing this distribution is the basis of land-use planning, environmental studies, disaster management, hydrological analysis, and water resources management [2–4]. However, the accuracy of the production of these maps depends on the methods used for the interpolation of the observed precipitation for the total considered area. Many different interpolation methods have been used in climate analysis so far [5–12], and finding the most suitable precipitation interpolation method is still a research desideratum for many regions [4,13–17].

Numerous studies were carried out in different regions on interpolation and estimation of precipitation and the selection of the best interpolation method. For example, for the Greater Sydney region of Australia, Ref [18] compared ANUDEM, Spline, Inverse Distance Weighting (IDW), and Kriging, and concluded that the IDW method showed the best performance. In the Qharesu Basin of northwestern Iran, Ref [19] examined Thiessen Polygons (THI), IDW, and Universal Kriging (UNK), and concluded that the THI method is most accurate in estimating precipitation and runoff in this basin. For annual precipitation zoning on the Tibetan Plateau, Ref [20] compared Ordinary Kriging, Co-Kriging with an auxiliary elevation variable, and Co-Kriging with an auxiliary Tropical Rainfall Measuring Mission (TRMM) variable. Their results show that the last method was the most effective one, and can be used as a new method for zoning precipitation in regions with a limited number of rain-gauge stations. In another study, Ref [21] used IDW, Radar value (Radar), Regression distance weighting (RIDW), Regression Kriging (RK), and Regression Co-Kriging (RCK) to estimate precipitation in the Alpine Basin, and showed that the RCK method had the best performance. In a study for northwestern China and the Qinghai Tibet Plateau, Ref [22] used the ANUSPLIN method for precipitation zoning. Considering that the precipitation of China is heavily influenced by its complex topography, they believe that the ANUSPLINE method, taking into account the effect of topography in estimating precipitation, could be a good method for zoning precipitation in this region. Generally, the quality of the applied interpolation methods strongly varied between the different study areas, demonstrating the need to individually test such methods for specific regions.

The arid to semi-arid Khorasan Razavi province in northeastern Iran is densely settled today, and is partly intensively used for agriculture [23,24]. However, that region is currently coping with drought-related problems and a general aridification trend [25,26]. Therefore, finding the most appropriate method for precipitation interpolation in dry lands such as our study area is very important. Precipitation is the most important and key atmospheric element in this area, which has many spatial and temporal dispersions. Furthermore, due to the lack of synoptic and rain gauge stations in the region, the existence of a suitable interpolation method that can accurately estimate the amount of precipitation in the region is of great value and importance. Therefore, a reliable spatial assessment of precipitation would be essential. However, for this region, the quality of different techniques for the interpolation of precipitation distribution had not been systematically studied thus far. Therefore, to fill this gap we compared five different interpolation techniques to identify the best interpolation method of annual precipitation for this region.

2. Materials and Methods

2.1. Study Area and Data Description

This study is focused on the Khorasan Razavi province in northeastern Iran that covers a total area of 118.854 km^2 (ca. 7% of Iran; Figure 1). The province is limited to the north and northeast by Turkmenistan, to the east by Afghanistan, to the west by the provinces of Yazd and Semnan, to the northwest by the North Khorasan province, and to the south by the South Khorasan province. A total of 49.2% of the province are mountain areas with altitudes between 231 and 3305 m a.s.l. Precipitation in this region ranges between 114.2 and 310.2 mm/a, and is linked with westerly disturbances [27].

For our study, we used annual rainfall data of 97 climate stations. We concentrated on the 20 years long period between 1994 and 2014 (annual data between 10th of October and 9th of October of the following year), since all stations showed complete data sets only for these consecutive years. The data were delivered by the Regional Water Organization and the Department of Climatology of the Khorasan Razavi province. Geographical locations and altitudes of the climate stations are shown in Table 1.

Table 1. Locations and altitudes of the meteorological stations used for this study.

Station	Longitude	Latitude	Altitude (m a.s.l.)	Station	Longitude	Latitude	Altitude (m a.s.l.)	Station	Longitude	Latitude	Altitude (m a.s.l.)
Emamzadeh-Mayamey	76°88′68″	40°35′25.1″	1039	Dolatabad Khoramdareh	69°31′77″	40°39′80.0″	1575	Khatiteh	51°74′98″	40°46′84.0″	1435
Balghoor	71°36′48″	40°67′52.4″	1941	Hey Hey Ghoochan	63°58′99″	41°08′34.3″	1344	Marosk	63°86′67″	40°43′51.6″	1525
Zoshk	72°69′04″	40°86′07.6″	1832	Sanobar	69°37′55″	39°21′18.2″	1707	Hendelabad	72°58′93″	39°89′92.5″	1206
Bakvol	69°52′22″	39°29′72.8″	1849	Namegh	65°96′98″	39°20′54.7″	1815	Hosseinabad	62°45′86″	39°88′70.7″	1072
Ghonchi	70°15′02″	39°32′19.3″	1892	Nari	73°96′95″	39°42′62.5″	1861	Karat	75°41′55″	38°75′63.2″	1084
Chakaneh Olya	72°70′59″	40°77′15.7″	1704	Kalateh Rahman	74°69′26″	39°62′05.3″	1619	Ghand e Jovein	53°61′66″	40°54′89.2″	1140
Darband Kalat	74°95′86′	40°78′20.3″	960	Sharifabad-Kashafrood	70°85′08″	40°21′00.1″	1467	Rashtkhar	63°18′58″	38°52′25.2″	1155
Dizbad	70°51′49″	39°97′75.9″	1988	Farhadgerd-Fariman	74°84′55″	39°40′39.7″	1503	Sangerd	60°30′34″	39°61′80.5″	1291
Archangan	74°26′34″	40°98′00.7″	757	Chahchaheh	73°11′33″	40°73′49.8″	486	Kalateh	71°40′70″	40°01′73.9″	983
Jang	67°64′01″	40°74′98.4″	2313	Dargaz	64°53′23″	41°64′51.6″	494	Sahlabad	73°06′76″	39°05′49.4″	1360
Mareshk	74°06′95″	40°56′09.3″	1830	Hatamghaleh	72°14′81″	41°12′76.6″	493	Irajabad	60°61′76″	39°03′17.0″	1041
Yengjeh abshar	61°27′00″	40°76′67.8″	1703	Ghand Torbat	70°14′68″	39°13′15.1″	1474	Ghand Torbatjam	75°75′41″	39°53′87.6″	888
Mohammad Taghi Beyg	62°84′49″	41°61′05.4″	1009	Ghare Shisheh	76′16″40°	39°37′56.5″	1512	Edareh Mashhad	69°70′23″	40°23′74.2″	1018
Talghor	67°63′94″	40°40′11.4″	1563	Beyroot	60°40′18″	39°51′53.0″	1452	Sharifabad	55°94′24″	39°10′36.0″	1100
Ferizi	67°40′19″	40°51′60.6″	1631	Andarokh	70°97′98″	40°30′68.6″	1207	Janatabad	71°01′54″	38°46′69.3″	925
Eishabad	66°43′19″	40°18′99.4″	1406	Sad Torogh	63°16′77″	40°78′32.1″	1242	Chenaran	74°30′31″	39°98′62.8″	1186
Saghbeig	62°67′89″	40°64′65.2″	1532	Karkhaneh Ghand	64°34′74″	40°17′69.6″	1207	Kashmar	63°26′35″	38°99′53.5″	1503
Taghoon	65°09′47″	40°32′14.9″	1503	Gharehtikan	72°49′66″	41°15′04.3″	527	Sabzevar	56°15′69″	40°08′14.9″	988
Kariz No	83°63′25″	38°93′23.1″	1798	Dahneh Shoor	59°61′67″	40°48′15.0″	1243	Gonabad	65°49′15″	38°01′27.5″	1117
Ardak	72°95′87″	40°06′13.2″	1320	Kariz Kashmar	61°79′71″	39°25′09.9″	1420	Darooneh	53°71′94″	38°92′74.1″	870
Kapkan	66°93′47″	41°24′35.3″	1437	Talkhbakhsh	66°83′64″	39°54′93.2″	1496	Mazinan	48°33′62″	40°19′47.1″	848
Moghan	69°05′38″	40°57′48.2″	1788	Sheikh Abolghasem	69°99′75″	39°01′17.0″	1320	Bezangan	81°94′49″	40°22′02.4″	1027
Goosh Bala	73°18′37″	40°30′50.6″	1569	Kartian	71°60′22″	40°20′75.1″	1240	Fadak	75°86′40″	38°50′12.3″	991
Agh Darband	75°24′70″	40°15′90.5″	602	Roohabad	66°71′86″	39°92′84.4″	1138	Shahrno Bakharz	80°31′88″	38°76′84.0″	1282
Tabarokabad	65°27′15″	41°17′00.7″	1510	Ghadirabad	71°05′44″	40°78′18.3″	1195	Sangar Sarakhs	87°71′56″	40°14′52.2″	343
Al	72°89′19″	40°66′63.3″	1464	Zarandeh	63°44′80″	40°37′28.0″	1403	Hesar Dargaz	71°17′68″	41°46′14.6″	289
Gardaneh Kalat	63°56′16″	37°80′69.7″	966	Mozdooran	73°80′58″	40°51′80.8″	927	Sad Kardeh	73°94′44″	40°56′′35.5′	1279
Golmakan	67°69′40″	40°39′72.8″	1440	Dereakht Toot	71°96′53″	40°71′55.5″	1254	Abghad Ferizi	67°59′48″	40°40′22.3″	1390
Sarasiab	73°10′51″	40°21′77.9″	1296	Malekabad	71°79′93″	38°90′87.3″	1195	Zirban Golestan	70°70′16″	40°21′26.9″	1434
Cheharbagh	65°41′56″	40°46′18.4″	1599	Emamzadeh-Radkan	74°02′51″	39°35′00.5″	1214	Fariman	75°74′80″	39°53′90.3″	1419
Taroosk	70°13′99″	39°27′39.7″	1704	Olang e Asadi	72°60′73″	40°05′93.0″	912	Timnak Sofla	82°65′63″	39°32′37.0″	1176
Fadiheh	67°46′92″	39°16′82.4″	1611	Bagh Sangan	78°82′12″	38°29′78.5″	937	Deh Menj	80°21′48″	38°79′86.7″	1273
Dahaneh Akhlamad	65°16′63″	40°78′63.2″	1467								

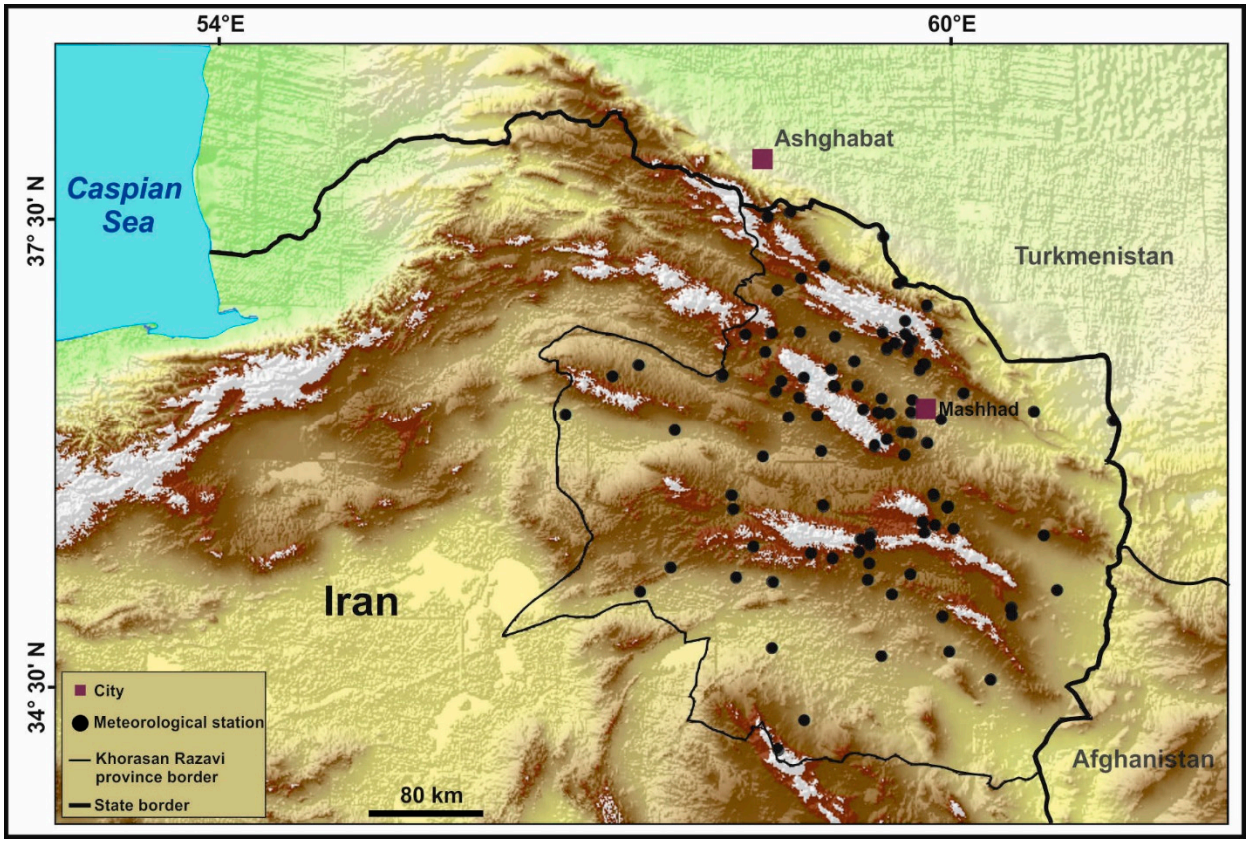

Figure 1. Location of the Khorasan Razavi province in Iran, and distribution of the meteorological stations used for this study (Map sources: Digital Elevation Model GTOPO30: https://earthexplorer.usgs.gov (accessed on 28 April 2021) and Digital Elevation Model ALOS PALSAR: https://vertex.daac.asf.alaska.edu (accessed on 28 April 2021)).

2.2. Methods

During this study, we tested five different interpolation methods to map annual precipitation in the Khorasan Razavi province that are described below. The models used include deterministic models (Inverse distance weighting and Radial basis function), geostatistical models (Kriging and Co-Kriging), and non-linear regression. The data were processed using GIS 10.5 and Curve Expert Pro Ver 2.6.5 software (Hyams Development, Alabama, United States).

2.2.1. Inverse Distance Weighting (IDW)

In the IDW method, the value of a single point is more strongly related to the nearby points around instead of points farther away. The equation is given by Equation (1):

$$Z_o = \frac{\sum_{i=1}^{s} Z_i \frac{1}{d_i^k}}{\sum_{i=1}^{s} \frac{1}{d_i^k}}. \quad (1)$$

Z_o is the estimated point o, Z_i is the value of Z at point i, d_i is the distance between points i and o, s is the number of points used in the estimate, and k is specified power. The power k controls the degree of local impact. A power of 1 means a constant amount of change in weighting of the known points with distance (linear interpolation), and a power of 2 or >2 indicates that the weighting of known points close to the point of interest is much greater than the distance would suggest. The degree of local impact also depends on the

number of known points that are used for the estimate. Some studies showed that a lower number of points (6 points) provides more favorable estimates than more points (12 points). The most important feature of the IDW method is that all predicted values range between the maximum and minimum known points [28].

2.2.2. Radial Basis Function (RBF)

RBF uses a generic function that depends on the distance between the points of interpolation and sampling [29]. The mathematical equation is given by Equation (2):

$$Z(x) = \sum_{i-1}^{n} a_i f_i(x) + \sum_{i-1}^{n} b_j \psi(d_j). \quad (2)$$

In this equation, $\psi(d)$ is the radial base function, and (d_j) shows the distance between the points of sampling and the predicted point x. $F(x)$ represents the process of the function and the fundamental member for polynomials with degrees less than m. The RBF calculations were based on the functions of Completely Regularized Spline (CRS), Spline with Tension (ST) and Multiquadric (MQ), Inverse Multiquadric (IMQ), and Thin Plate Spline (TPS). All equations are given below in Equations (3)–(7).

$$CRS \;\; \psi(d) = \ln(\frac{cd^2}{2}) + E_1(cd)^2 + y \quad (3)$$

$$ST: \quad \psi(d) = \ln(\frac{cd}{2}) + I_0(cd) + \gamma \quad (4)$$

$$MQ: \quad \psi(d) = (\sqrt{d^2 + c^2}) \quad (5)$$

$$IMQ: \quad \psi(d) = (\sqrt{d^2 + c^2})^{-1} \quad (6)$$

$$TPS: \quad \psi(d) = c^2 d^2 \ln(cd) \quad (7)$$

d: Is the distance from sample to prediction location
c: Is a smoothing factor
$I_0()$: Is the modified Bessel function
E: Euler's constant [30].

2.2.3. Kriging Method

Kriging differs from the other interpolation methods, because it can determine the quality of interpolation with the magnitude of error that occurred in predicting values. The Kriging method uses a semi-variogram to measure the spatially related component or spatial self-correlation (Please see the explanation of the semi-variogram in Appendix A). Kriging is calculated as given below in Equation (8):

$$\hat{Z}(x_0) - \mu = \sum_{i=1}^{N} \omega_i [Z(x_i) - \mu(x_0)]. \quad (8)$$

Here, $\hat{Z}(x_0)$ is the estimated random field (prediction attribute) value at point x_0, and μ is the stationary mean treated as constant over the whole region of interest (RoI). The parameter ω_i is the weight assigned to the ith interpolating point calculated from the semi variogram, and $Z(x_i)$ is the measured attribute value at a point x_i [31].

If there is a spatial dependence in the dataset, the points of contact that are close to each other must have a lower semi-variance compared with more distant points. Ordinary Kriging (OK), Universal Kriging (UK), and Simple Kriging (SK) are the Kriging methods that are used in this research. The difference between OK and SK is the assumption of stationarity, which expects the mean and distribution to remain constant throughout the region. SK utilizes this assumption while OK does not, and instead recalculates the mean

across the modeled area by a shifting search radius. But in reality, the mean value of some spatial data cannot be assumed to be constant in general but varies, since it also depends on the absolute location of the sample. For this sake, we use the UK method aiming to predict $Z(x)$ at unsampled places as well [32,33]. One precondition for using Kriging methods is the normalization of the data, or at least a near normally distributed dataset so that this method can give the best estimate with the lowest error coefficient. Here we used the log-normal method for normalization.

2.2.4. Co-Kriging Method

Co-Kriging is a multivariate version of Kriging that uses the spatial correlation between the primary variable (annual precipitation) and an auxiliary variable (here the elevations of the gauging stations) to estimate the main variable. Similar to the Kriging method, Ordinary Co-Kriging (OCo-K), Universal Co-Kriging (UCo-K), and Simple Co-Kriging (SCo-K) are used here. In Co-Kriging, along with calculating the semi variogram of the primary and secondary variable, it is necessary to calculate the cross semi-variogram that expresses the spatial correlation between those two variables (Please see the explanation of the semi-variogram in the Appendix B). The Co-Kriging equation (Equation (9)) is as follows:

$$Z*(x_i) = \sum_{i=1}^{n} \lambda_i Z(x_i) \sum_{k=1}^{n} \lambda_k U(x_k). \quad (9)$$

In this equation, λ_i is the weight of the main Z variable in x_i position, λ_k is the weight of the U auxiliary variable in x_k position, and $U(x_k)$ is the observed value of the x_k auxiliary variable in the position [34].

2.2.5. Non-Linear Regression

Non-linear regression analysis enables us to predict the changes of dependent variables through independent variables, and the contribution of every independent variable is determined by the presentation of a dependent variable [35]. Similar to Co-Kriging, we selected elevation as an independent variable, since this factor generally has a significant effect on the amount of precipitation. For interpolation using non-linear regression methods, first appropriate regression models have to be determined. This is achieved by calculating the degrees of correlation between the selected dependent and independent variables for several potential models. To find the best model for precipitation zoning in the study area, 69 non-linear regression models were evaluated (please see a list of all models in Table S1 of Supplementary Material). From these we selected the Sinusoidal, Hoerl, and Steinhart-Hart equations, since these gave the highest correlations between annual precipitation and elevation. The equations and coefficients of these selected models are as follows:

Equation (10) and Coefficients of Sinusoidal regression:

$$\begin{aligned} y &= a + b\cos(cx + d) \\ a &= 259.660192 \\ b &= 69.766364 \\ c &= 0.002285 \\ d &= 1.056829 \end{aligned} \quad (10)$$

Equation (11) and Coefficients of Hoerl regression:

$$\begin{aligned} y &= ab^x x^c \\ a &= 9080.760939 \\ b &= 1.000938 \\ c &= -0.688939 \end{aligned} \quad (11)$$

Equation (12) and coefficients of Steinhart-Hart equation regression:

$$\begin{array}{l} y = \frac{1}{a + b\ln(x) + c(\ln(x))^3} \\ a = -0.039299 \\ b = 0.010284 \\ c = -0.000081 \end{array} \quad (12)$$

The values of x in Equations (10)–(12) are the station elevation data taken from the Khorasan Razavi province Meteorology Organization and the digital elevation model (DEM) of the studied region (GTOPO30: https://earthexplorer.usgs.gov (accessed on 28 April 2021) and ALOS PALSAR: https://vertex.daac.asf.alaska.edu (accessed on 28 April 2021)).

2.2.6. Validation Criteria for the Applied Methods

There are various criteria for validating interpolation methods, with one of the most important being k-fold cross-validation [36]. This method estimates a value for every observation point by means of interpolation. Subsequently, the estimated value is compared with the observed value, and the model with the least error is regarded as the superior one. There are various ways to compare estimated and observed values, and the most important ones include Root Mean Square Error (RMSE), Mean Absolute Error (MAE), and the Coefficient of Determination (R^2) [37–40]. The equations to calculate RMSE (Equation (13)), (MAE) (Equation (14)), and R^2 (Equation (15)) are given below:

$$RMSE = \sqrt{\frac{1}{n}\sum_{i=1}^{n_v}(z(x_i) - \hat{z}(x_i))^2} \quad (13)$$

$$MAE = \frac{1}{n_v}\sum_{i=1}^{n_v}|z(x_i) - \hat{z}(x_i)| \quad (14)$$

$$R^2 = \frac{\sum_{n=1}^{n} X_n Y_n}{\sqrt{\sum_{n=1}^{n} X_{n^2} \sum Y_{n^2}}}. \quad (15)$$

In Equations (13) and (14), $z(x_i)$ is the observed value, $\hat{z}(x_i)$ is the estimated value and n is the number of sites. In Equation (15), X_n is the observed amount, Y_n is the estimated amount and n is the number of data. Lower values of MAE and RMSE and higher values of R^2 indicate a better performance of the interpolation method. In case of a very precise estimator, MAE and RMSE would be zero, and R^2would be 1.

3. Results

3.1. General Statistics

Table 2 shows the descriptive statistics of the annual precipitation data of the studied gauging stations. According to that table, average annual precipitation in the study area is 229.77 mm. The coefficient of variation (CV) is 25.67 mm, indicating a relatively low spatial variation of regional precipitation. Furthermore, that low CV value also indicates the absence of large outliers in the regional dataset.

Table 2. Descriptive statistics of 20-year mean annual precipitation data of the Khorasan Razavi province 1994–2014.

Min	Max	Mean	Std.Dev	Skewness	Kurtosis	CV
137	400	229.77	58.081	0.131	2.44	25.669

3.2. Interpolation Methods

3.2.1. Inverse Distance Weighting (IDW)

Based on the results of the cross-validation, the parameters (k) and maximum and minimum number of neighborhood points (s) were optimized to minimize RMSE and MAE. Doing so, a power (k) of 1, a minimum number of neighborhood points of 2 and a maximum number of 6 neighborhood points gave the lowest possible error values of 53.07 for RMSE and of 1.108 for MAE, and the highest value for of 0.166, respectively. The resulting interpolated annual precipitation map of the Khorasan Razavi province is shown in Figure 2.

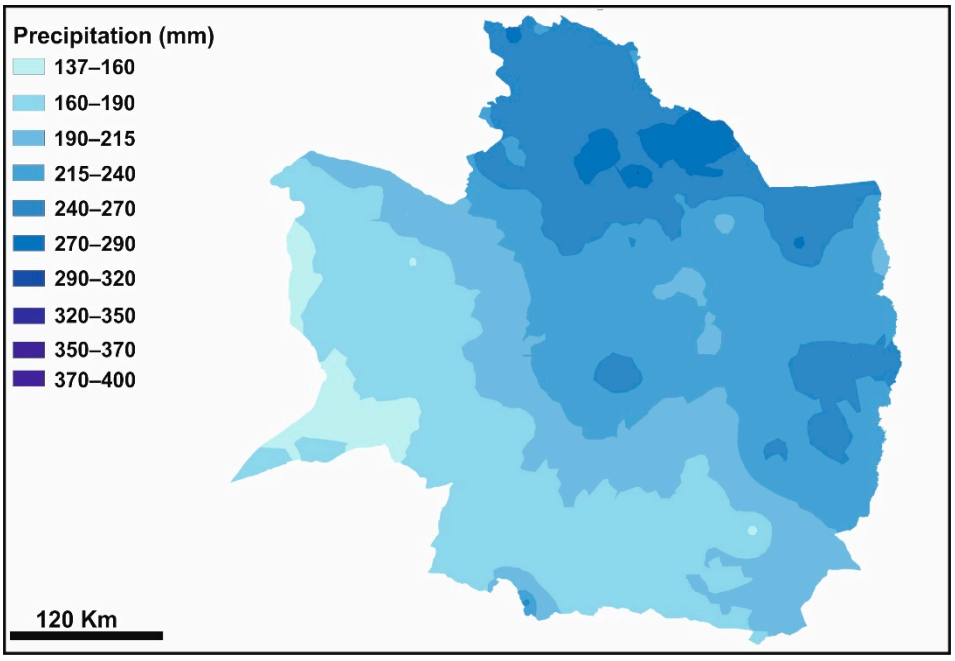

Figure 2. Interpolated annual precipitation map based on the IDW method.

3.2.2. Radial Basis Function (RBF)

Of the five Radial Basis Functions that were evaluated, Spline with Tension showed the lowest RMSE error, an intermediate MAE error, and the highest R^2 value, and therefore turned out to be the best method (Table 3). It should be noted that the number of neighboring points was at least 2 and at most 8, and for optimizing and minimizing the estimation errors [41], the Kernel function 5/195387 was used. Interpolated annual precipitation maps of the Khorasan Razavi province derived from the five RBF functions are shown in Figure 3.

Table 3. Error values and R^2 for the five applied RBF methods.

Method	RMSE	MAE	R^2
Completely Regularized Spline	52.57	1.120	0.177
Spline with Tension	52.46	1.116	0.179
Multiquadric	61.21	1.515	0.098
Inverse Multiquadric	53.39	1.060	0.147
Thin Plate Spline	270.87	2.490	0.048

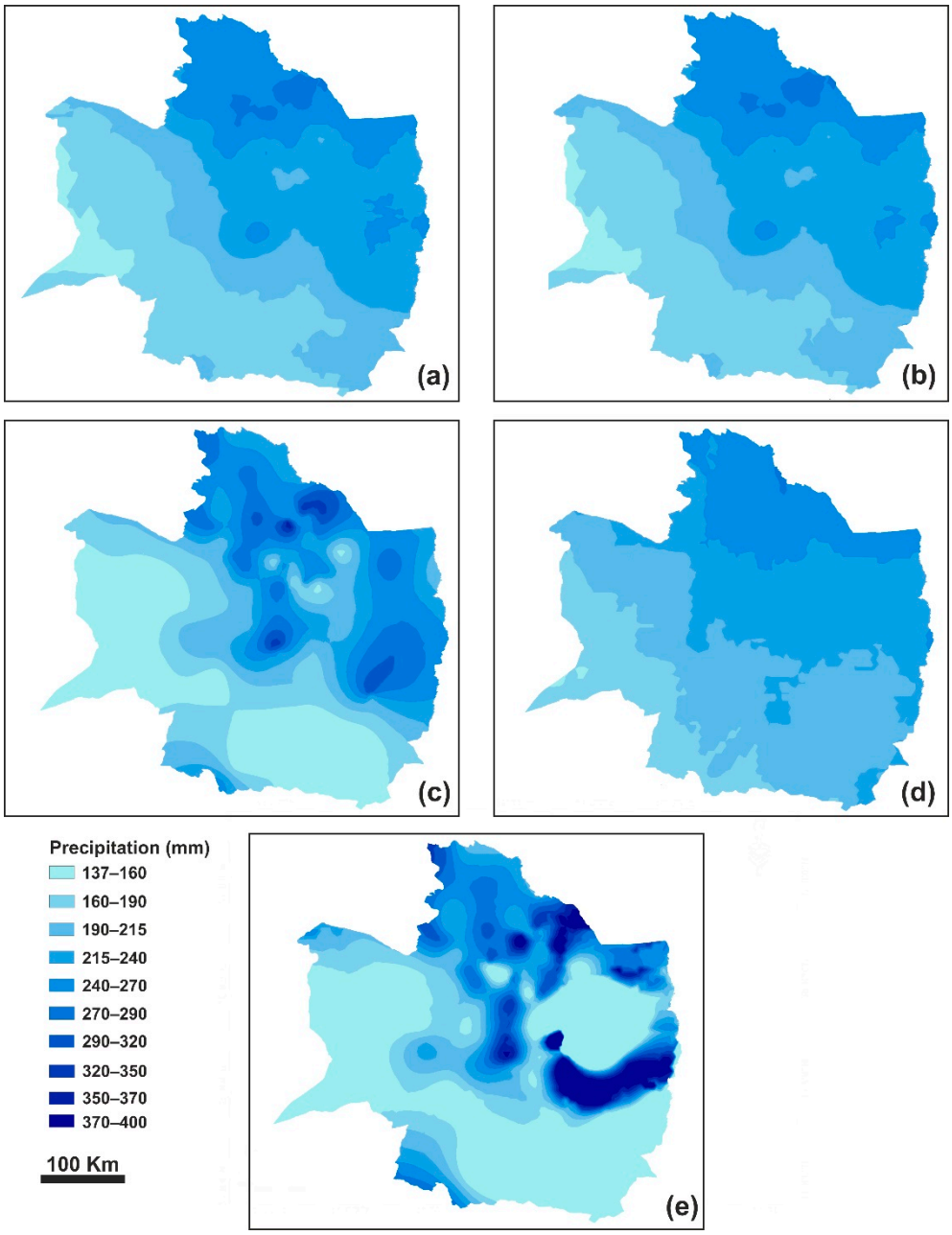

Figure 3. Interpolated annual precipitation maps based on the five Radial Basis Functions: (**a**) Completely Regularized Spline, (**b**) Spline with Tension, (**c**) Multiquadric, (**d**) Inverse Multiquadric, (**e**) Thin-Plate Spline.

3.2.3. Kriging

Ordinary, Universal, and Simple Kriging methods were used in this study. The results of the cross-validation show that Simple Kriging (SK) had the largest MAE error but the least RMSE error and the highest coefficient of determination, and therefore turned out to be the best method (Table 4). In order to achieve the best estimate with the SK method, we used the Hole Effect's theoretical model to fit the semi-variogram with a maximum of 6 neighborhoods. The interpolated annual precipitation maps of the Khorasan Razavi province derived from the three applied Kriging methods are shown in Figure 4.

Table 4. Error values and R^2 for the three applied Kriging methods.

Method	Semi-Variogram Theoretical Model (Appendix A)	RMSE	MAE	R^2
Ordinary (OK)	Circular	51.33	1.128	0.211
Simple (SK)	Hole Effect	50.90	1.145	0.224
Universal (UK)	Exponential	51.33	1.128	0.211

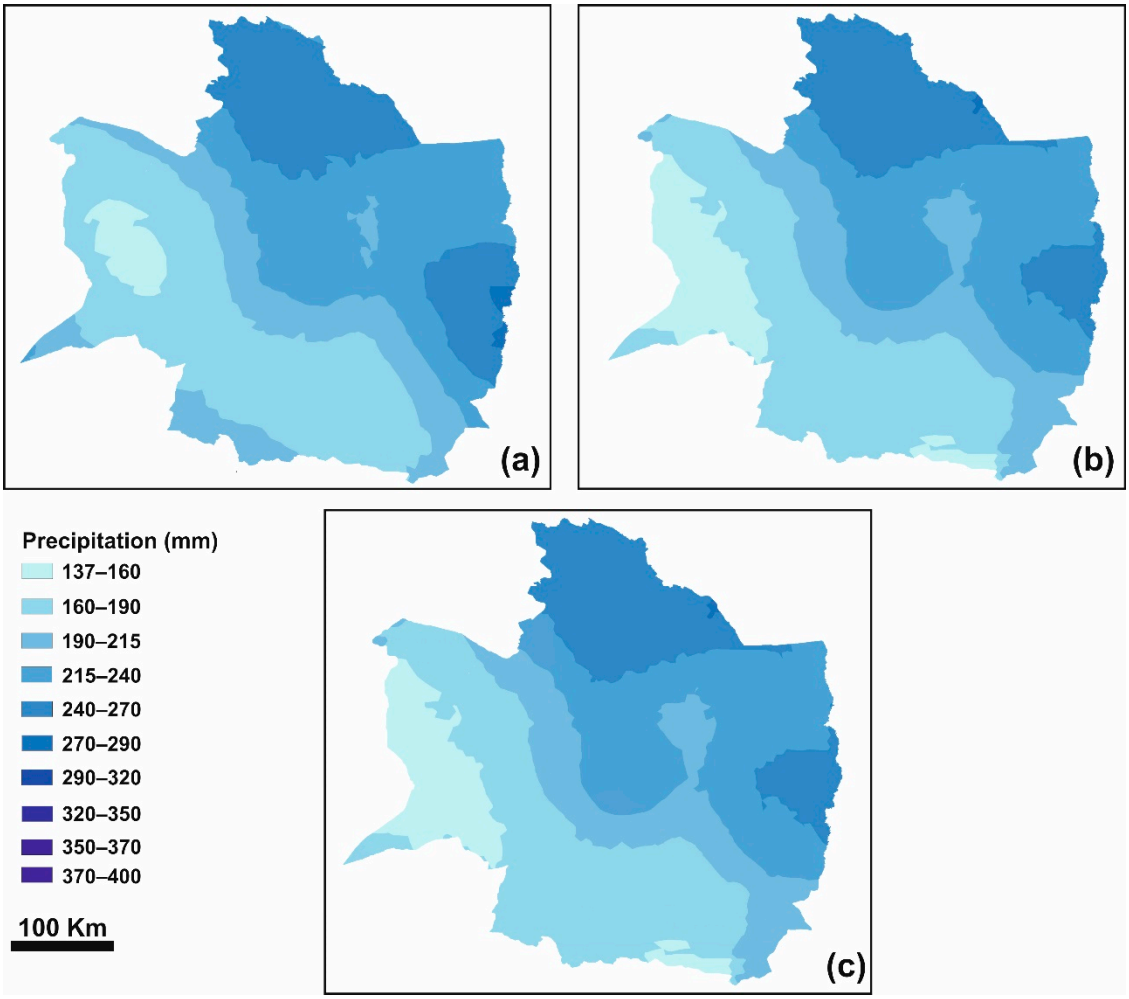

Figure 4. Interpolated annual precipitation maps based on the three Kriging methods: (**a**) Simple, (**b**) Ordinary, (**c**) Universal.

3.2.4. Co-Kriging

Given that Co-Kriging generally uses an auxiliary parameter, we used the elevation as such an effective auxiliary parameter for precipitation interpolation in the Khorasan Razavi province. Simple (SCoK), Ordinary (OCoK), and Universal (UCoK) Co-Kriging were compared with each other. Despite showing a higher MAE error compared with SCoK, OCoK and UCoK showed the lowest and identical RMSE errors and the highest and identical R^2 values (Table 5). Therefore, OCoK and UCoK turned out to be the best Co-Kriging methods. The interpolated annual precipitation maps of the Khorasan Razavi province derived from the three Co-Kriging methods are shown in Figure 5.

Table 5. Error values and R^2 for the three applied Co-Kriging methods.

Method	Cross Semi-Variogram Theoretical Model	RMSE	MAE	R^2
OCoK	K-Bessel	42.18	1.108	0.468
SCoK	K-Bessel	45.45	0.777	0.377
UCoK	Exponential	42.18	1.108	0.468

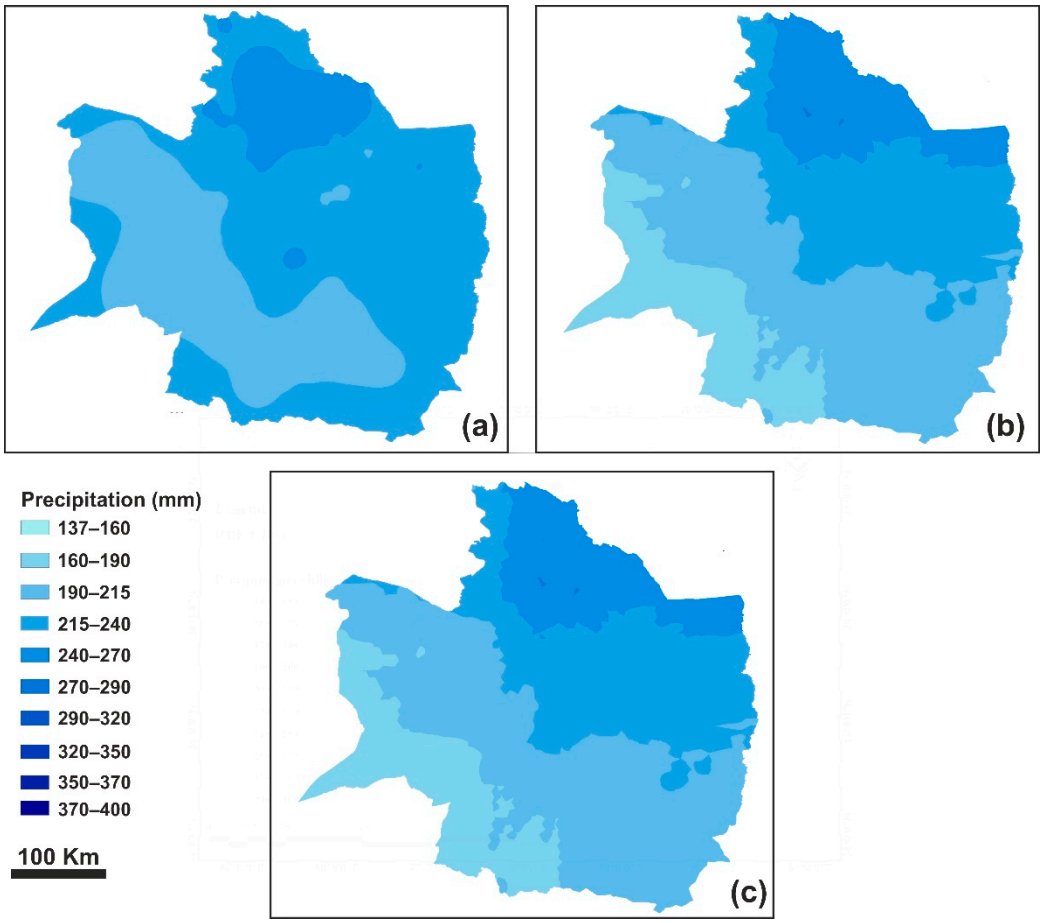

Figure 5. Interpolated annual precipitation maps based on the three Co-Kriging methods: (**a**) Simple, (**b**) Ordinary, (**c**) Universal.

3.2.5. Non-Linear Regression Method

According to our preceding analysis, the best non-linear regression models with respect to annual precipitation and elevation data in the study area are the Sinusoidal, Hoerl, and Steinhart-Hart equations, since these show the highest correlations between annual precipitation as the dependent and elevation as the independent variable: The correlations were 0.607, 0.576, and 0.566, and the R^2 values were 0.364, 0.332, and 0.324, respectively. In Figure 6, the regression lines of the three different non-linear regression methods are shown in a scatter plot that displays altitude and annual precipitation of the gauging stations in the study area.

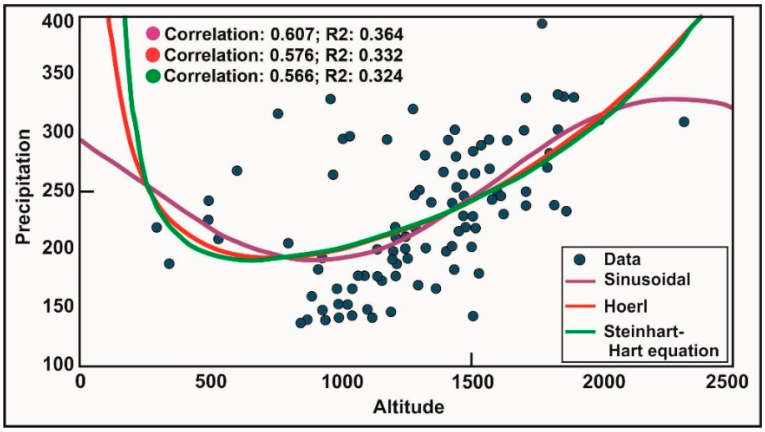

Figure 6. Scatter plot displaying altitude and annual precipitation data of the gauging stations in the study area, and the regression lines of the three applied non-linear regression methods.

In order to integrate altitudinal zoning, equations and correlation coefficients of the three models were combined with the digital elevation model (DEM) of the study area, resulting in interpolated annual precipitation maps of the Khorasan Razavi province (Figure 7).

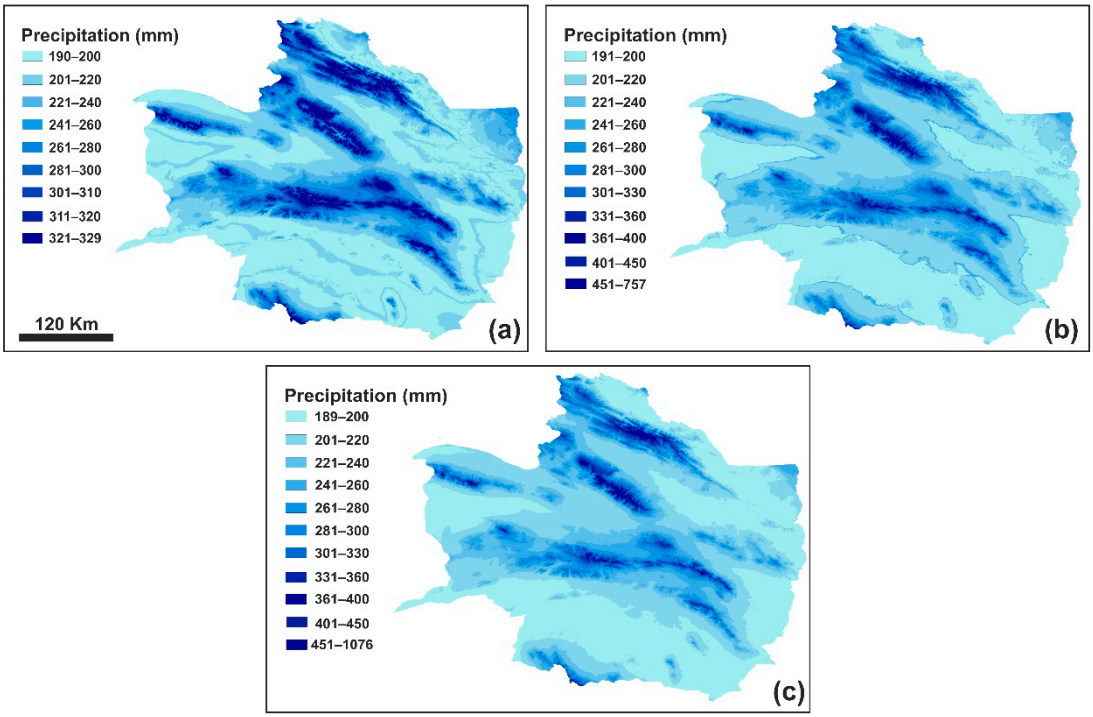

Figure 7. Interpolated annual precipitation maps obtained by applying the three non-linear regression methods: (**a**) Sinosoidal, (**b**) Hoerl, (**c**) Steinhart-Hart Equation. Please note that the individual maps have different precipitation scales.

According to the cross-validation, on the one hand the Sinusoidal model shows the highest RMSE and MAE errors, but on the other hand it shows the highest R^2 value of all non-linear regression models (Table 6). As can be seen by the regression lines in Figure 6, maximal annual precipitation calculated with the Hoerl and Steinhart-Hart equations is much higher than that calculated with the Sinusoidal model, resulting in values for maximal annual precipitation of 757 mm (Hoerl) and 1076 mm (Steinhart-Hart) compared with 329 mm (Sinusoidal). By comparing the calculated values of these three models with the observed data (Figure 6), it can be seen that the Hoerl and Steinhart-Hart models have

estimated 357 and 676 mm more than the highest measured amount of precipitation in the region, respectively, whereas the Sinusoidal model has estimated 71 mm less than the actual amount of observed precipitation in the region. Therefore, it can be concluded that the amount of precipitation estimated by the Sinusoidal model is closer to reality, so that this model was selected for further evaluation.

Table 6. Errors and correlations between observed and estimated annual precipitation amounts of the three selected non-linear regression methods.

Method	RMSE	MAE	R^2
Sinusoidal	56.73	1.477	0.119
Hoerl	56.37	0.707	0.111
Steinhart-Hart Equation	55.63	0.699	0.110

4. Discussion

The results of the analysis for the five compared interpolation methods are comparatively shown in Table 7 and Figure 8 (in case of several sub-methods the result(s) of the best-performing method(s) was/were selected). Ordinary and Universal Co-Kriging showed the lowest errors with an R^2 value of 0.469, as well as showing the highest R^2 values of all methods, and therefore gave the most correct results of interpolation for the Khorasan Razavi province. Among the deterministic and geostatistical methods, with an R^2 value of just 0.166, IDW seems to be the worst method for annual precipitation interpolation in the Khorasan Razavi province. However, with an R^2 value of 0.119, the (best-performing) regression method with Sinusoidal function gave the worst annual precipitation estimation in the study area of all methods.

Table 7. Errors and correlations between observed and estimated annual precipitation amounts of the compared five methods.

Method (in the Case of Several Sub-Methods, the Best-Performing One Was Selected)	RMSE	MAE	R^2
IDW	53.07	1.108	0.166
RBF (Spline with Tension)	52.46	1.116	0.179
Kriging (Simple Kriging)	50.90	1.145	0.220
Co-Kriging (Ordinary and Universal Co-Kriging)	42.18	1.108	0.469
Non-linear regression (Sinusoidal)	56.73	1.477	0.119

Generally, due to the regular application of altitude as an auxiliary elevation variable when estimating precipitation for an area, in the case of a missing high correlation between elevation and precipitation regression methods are not capable of interpolating precipitation with high accuracy. In our present study, the average correlation between annual precipitation and elevation of the best-performing Sinusoidal function was only 60% (Figure 7). Therefore, our precipitation estimation using regression models was very weak (Table 7). The observed low correlation between annual precipitation and elevation could be due to: (i) The lack of rain gauge and synoptic stations at altitudes above 2313 m a.s.l. led to a lack of observational data for these higher regions. Therefore, the model has to determine precipitation for these altitudes using recorded data from lower altitudes, what decreases the general accuracy of this model; (ii) An unequal distribution of observation stations in the area (Figure 1); (iii) Luff-lee effects, leading to different precipitation amounts upwind and downwind of moisture-laden airflow at similar altitudes. Similarly, also during former studies, it was found that in case of a low correlation between annual precipitation and elevation regression models show rather bad results compared with the Kriging and Co-Kriging methods [42–44].

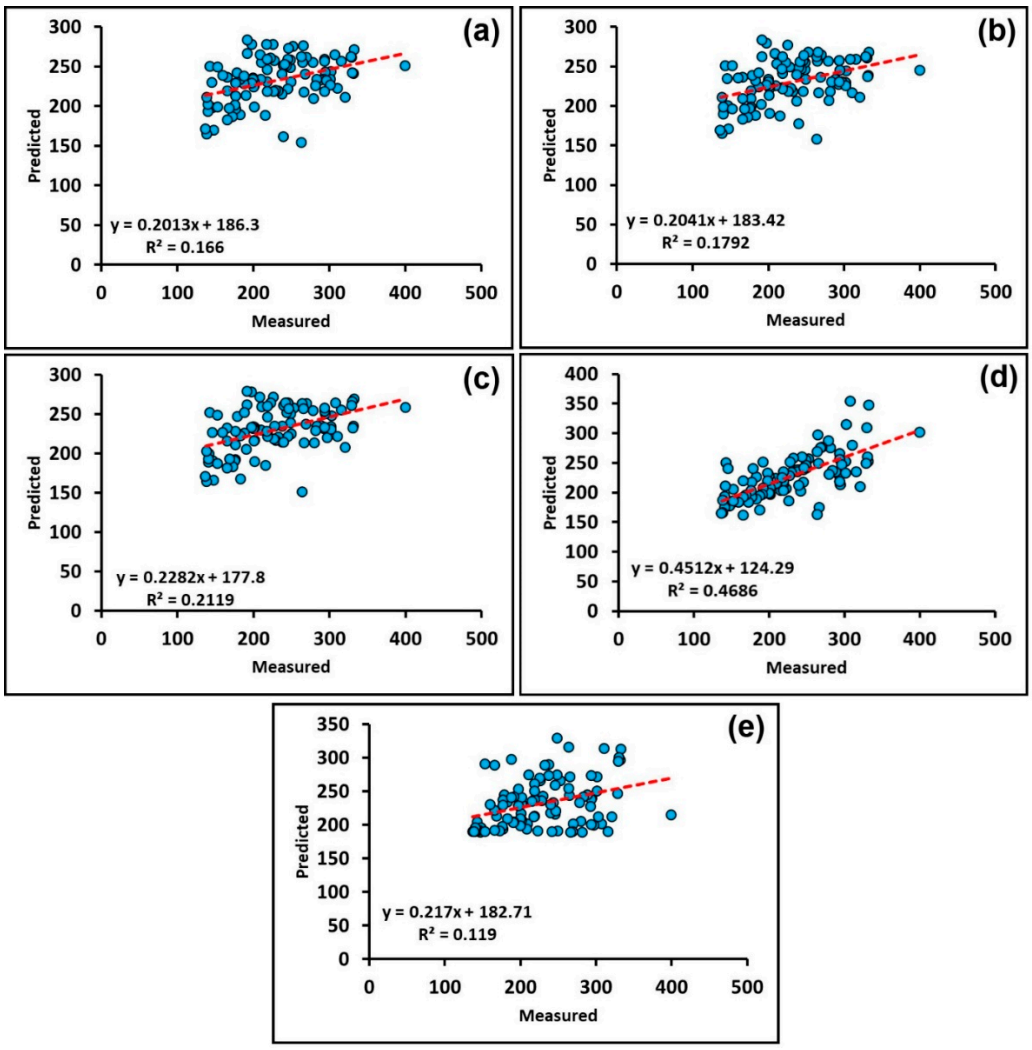

Figure 8. Scatter plot of measured and predicted amounts of annual precipitation of the compared five interpolation methods. (**a**) IDW, (**b**) RBF: Spline with Tension, (**c**) Kriging: Simple Kriging, (**d**) Co-Kriging: Ordinary Co-Kriging, (**e**) Non-linear regression: Sinusoidal equation.

Generally, there is no model that can decisively be selected as the best one for all regions. With respect to Iran, for some regions with a high correlation between precipitation and elevation, regression models turned out to be the best [4,14–17], whereas in most regions, Kriging and Co-Kriging gave more accurate results compared with the other methods [15,16,20]. Similarly, despite some studies describing IDW as the best method [45–47], many studies emphasize the high accuracy of geostatistical methods (Kriging and Co-Kriging) for precipitation estimation for other regions as well, with Co-Kriging using the auxiliary elevation variable often showing the highest accuracy [9,12,48–55]. Similar to in the above-mentioned studies, also during this study an acceptable accuracy of (Ordinary and Universal) Co-Kriging, using the auxiliary elevation variable, was found. Unlike regression models that only use elevation as an auxiliary parameter, Co-Kriging takes into account the autocorrelation factor and the statistical relationship between data in the region, leading to more reliable estimates compared with regression methods.

The annual precipitation map obtained by ordinary Co-Kriging shows highest annual precipitation concentrated in the mountainous northern part of the province. In contrast, in the southern and western part, showing lower altitudes, annual precipitation decreases. Corresponding with this natural water supply, the population density of the province decreases from North to South (Figure 9). Generally, finding a suitable method

for interpolating and estimating precipitation in an area can have many applications based on different aspects. On the one hand, the accurate interpolation of precipitation can be of great help for land-use planners to allocate suitable agricultural, industrial, tourist, residential and other uses. On the other hand, for controlling and managing natural and environmental disasters such as floods, dust phenomena, landslides, desertification, deforestation, etc., which are directly and indirectly related to the amount of precipitation in the region, accurate estimations of precipitation can be very useful and effective. Consequently, an accurate interpolation of precipitation in a region provides decision-makers with a comprehensive view of precipitation conditions, which can be used to plan well and control water resources. Therefore, finding a suitable model for accurate spatial estimation of precipitation in the arid to semi-arid study area, which is always in crisis in terms of precipitation, is a major challenge.

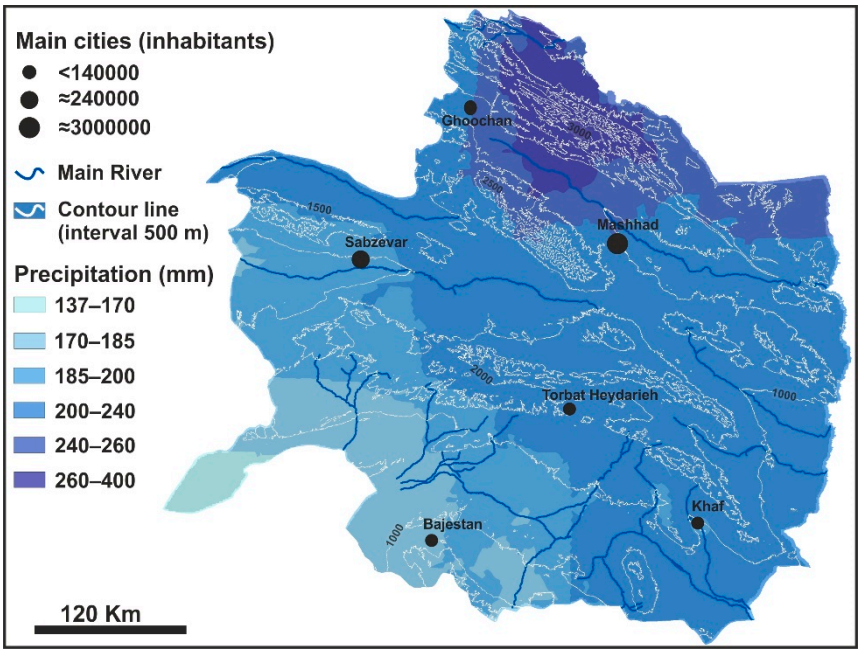

Figure 9. Annual precipitation Map of Khorasan Razavi province interpolated by Ordinary Co-Kriging, main streams and main settlements combined with the main contour lines of a DEM (Map sources: Digital Elevation Model GTOPO30: https://earthexplorer.usgs.gov (accessed on 28 April 2021)).

5. Conclusions

The precipitation map is a main database for environmental issues and studies such as disaster management, hydrological analysis, agricultural management, etc. Therefore, figuring out an accurate interpolation method to estimate the distribution of precipitation in regions that largely lack synoptic and rain gauge stations is an urgent task. During this study, for the first time we systematically compared five different methods to interpolate annual precipitation for the Khorasan Razavi province in northeastern Iran. This should allow extensive simulations of regional precipitation with high confidence. Similar to former studies, our results showed that with a coefficient of determination of 46.9% Ordinary Co-Kriging, also taking into account elevation, gave the most reliable results. In contrast, regression methods showed the largest errors and lowest coefficient of determination of only 12%. Therefore, our study suggests that the application of precipitation mapping using Ordinary Co-Kriging with an auxiliary elevation variable would form a mandatory base for future water supply-related regional planning and policy making in the Khorasan Razavi province. This holds especially true against the background of the current global climate change leading to a regional aridification trend in this province, and given its

partly high population density and intensive agriculture. It should be noted that the results obtained from this study can be applied not only in this region, but also in neighboring areas with similar environmental conditions.

Supplementary Materials: The following is available online at https://www.mdpi.com/article/10.3390/atmos12050592/s1, Table S1: List of the tested non-linear regression models.

Author Contributions: Conceptualization, M.A. and A.K.; methodology, M.A. and A.K.; investigation, M.A. and A.K.; writing—original draft preparation, M.A. and A.K.; writing—review and editing, M.A. and A.K.; visualization, M.A. and A.K. All authors have read and agreed to the published version of the manuscript.

Funding: This research received no external funding.

Institutional Review Board Statement: Not applicable.

Informed Consent Statement: Not applicable.

Data Availability Statement: Data sharing not applicable.

Acknowledgments: The authors owe their gratitude to the responsible authorities of the Regional Water Organization, and the Meteorological Organization of Khorasan Razavi Province for providing the data for this research, and to Tim Kerr (National Institute of Water and Atmospheric Research, Christchurch, New Zealand) for his careful reading of the manuscript and constructive comments. Furthermore, we thank two anonymous reviewers for their valuable comments on a first version of this manuscript.

Conflicts of Interest: The authors declare no conflict of interest.

Appendix A

Semi-Variogram

One of the common geostatistical tools to investigate spatial changes of climatic elements is the semi-variogram. The semi variogram indicates the dissimilarity between the values of a feature when the distance between the samples increases. For accurate estimation and minimization of estimates performed by the semi-variogram, eleven models including Circular, Spherical, Tetra-spherical, Penra-spherical, Exponential, Gaussian, Rational Quadratic, Hole Effect, K-Bessel, J-Bessel, and Stable are used. It should be noted that from these models that one with the best fit with the data is selected and used for the estimation process. In practice, the semi-variogram is equal to half of the mean square of the difference between the amounts of each pair of points located at a distance h from each other:

$$y^*(h) = \frac{1}{2n(h)} \sum_{i=1}^{n(h)} [Z(x_i) - Z(x_i + h)]^2 \quad \text{(A1)}$$

In this equation, $y^*(h)$ is the semi-variogram, $n(h)$ denotes the total number of pairs of observation points with distance h, $Z(x_i)$ the observed amount of the variable Z in position x_i, and $Z(x_i + h)$ is the measured attribute value at the point which is separated by lag distance h from x_i [40].

Appendix B

Cross Semi-Variogram

In some cases, data of other variables are available for the same locations or exist in larger numbers than the primary variable, and the primary and secondary variable are well correlated with each other. In such cases the accuracy of estimating the primary variable can be improved by using the Co-Kriging method that uses data related to the primary or secondary variable. In this method, next to calculating the semi variogram of the primary and secondary variable, it is necessary to calculate the cross semi-variogram that expresses

the spatial correlation between those two variables. The cross semi-variogram is calculated as follows:

$$y^*_{v,w}(h) = \frac{1}{2n(h)}\sum_{i=1}^{n}(Z_v(x_i) - Z_v(x_i+h)(Z_w(x_i) - Z_w(x_i+h))) \quad \text{(A2)}$$

In this equation, $y^*_{v,w}(h)$ is the experimental cross semi-variogram, $n(h)$ the total number of pairs of observation points with distance h, $Z_v(x_i)$ the amount of the observed variable Z_v in position x_i, $Z_v(x_i+h)$ the amount of the observed variable Z_v in position x_i+h, $Z_w(x_i)$ the amount of the observed variable Z_w in position x_i, and $Z_w(x_i+h)$ the amount of the observed variable Z_w in position x_i+h. Whereas the semi-variogram should always be positive by definition, the cross semi-variogram can be negative when the relationship between the two variables is negative [56].

References

1. Greco, A.; De Luca, D.L.; Avolio, E. Heavy precipitation systems in Calabria Region (Southern Italy): High-resolution observed rainfall and large-scale atmospheric pattern analysis. *Water* **2020**, *12*, 1468. [CrossRef]
2. Taesombat, W.; Sriwongsitanon, N. Areal rainfall estimation using spatial interpolation techniques. *Sci. Asia* **2009**, *35*, 268–275. [CrossRef]
3. Jun, L. Development of Isohyet Map Using Inverse Distance Weighting and Ordinary Kriging Methods. Bachelor Thesis, Faculty of Civil Engineering and Earth Resources, University of Malaysia Pahang, Pahang, Malaysia, 2018.
4. González-Álvarez, Á.; Viloria-Marimón, O.M.; Coronado-Hernández, Ó.E.; Vélez-Pereira, A.M.; Tesfagiorgis, K.; Coronado-Hernández, J.R. Isohyetal maps of daily maximum rainfall for different return periods for the Colombian Caribbean Region. *Water* **2019**, *11*, 358. [CrossRef]
5. Ly, S.; Charles, C.; Degre, A. Geostatistical interpolation of daily rainfall at catchment scale: The use of several variogram models in the Ourthe and Ambleve catchments, Belgium. *Hydrol. Earth Syst. Sci.* **2011**, *15*, 2259–2274. [CrossRef]
6. Matos, J.P.; Liechti, T.C.; Portela, M.M.; Schleiss, A.J. Pattern-oriented memory interpolation of sparse historical rainfall records. *J. Hydrol.* **2014**, *510*, 493–503. [CrossRef]
7. Zhang, Y.; Vaze, J.; Chiew, F.H.; Teng, J.; Li, M. Predicting hydrological signatures in ungauged catchments using spatial interpolation, index model, and rainfall–runoff modelling. *J. Hydrol.* **2014**, *517*, 936–948. [CrossRef]
8. Nikolopoulos, E.I.; Borga, M.; Creutin, J.D.; Marra, F. Estimation of debris flow triggering rainfall: Influence of rain gauge density and interpolation methods. *Geomorphology* **2015**, *243*, 40–50. [CrossRef]
9. Plouffe, C.C.; Robertson, C.; Chandrapala, L. Comparing interpolation techniques for monthly rainfall mapping using multiple evaluation criteria and auxiliary data sources: A case study of Sri Lanka. *Environ. Modell. Softw.* **2015**, *67*, 57–71. [CrossRef]
10. Zhang, T.; Xu, X.; Xu, S. Method of establishing an underwater digital elevation terrain based on kriging interpolation. *Measurement* **2015**, *63*, 287–298. [CrossRef]
11. Bhunia, G.S.; Shit, P.K.; Maiti, R. Comparison of GIS-based interpolation methods for spatial distribution of soil organic carbon (SOC). *J. Saudi Soc. Agric. Sci.* **2016**, *17*, 114–126. [CrossRef]
12. Mendez, M.; Calvo-Valverde, L. Assessing the performance of several rainfall interpolation methods as evaluated by a conceptual hydrological model. *Procedia Eng.* **2016**, *154*, 1050–1057. [CrossRef]
13. Caruso, C.; Quarta, F. Interpolation methods comparison. *Comput. Math. Appl.* **1998**, *35*, 109–126. [CrossRef]
14. Chen, T.; Ren, L.; Yuan, F.; Yang, X.; Jiang, S.; Tang, T.; Zhang, L. Comparison of spatial interpolation schemes for rainfall data and application in hydrological modeling. *Water* **2017**, *9*, 342. [CrossRef]
15. İçağa, Y.; Emin, T.A.Ş. Comparative Analysis of Different Interpolation Methods in Modeling Spatial Distribution of Monthly Precipitation. *Doğal Afetler ve Çevre Dergisi* **2018**, *4*, 89–104. [CrossRef]
16. Huang, H.; Liang, Z.; Li, B.; Wang, D. A new spatial precipitation interpolation method based on the information diffusion principle. *Stoch. Environ. Res. Risk Assess.* **2019**, *33*, 765–777. [CrossRef]
17. Liu, D.; Zhao, Q.; Fu, D.; Guo, S.; Liu, P.; Zeng, Y. Comparison of spatial interpolation methods for the estimation of precipitation patterns at different time scales to improve the accuracy of discharge simulations. *Hydrol. Res.* **2020**, *51*, 583–601. [CrossRef]
18. Yang, X.; Xie, X.; Liu, D.L.; Ji, F.; Wang, L. Spatial Interpolation of Daily Rainfall Data for Local Climate Impact Assessment over Greater Sydney Region. *Adv. Meteorol.* **2015**, *2015*, 563629. [CrossRef]
19. Zeinivand, H. Comparison of interpolation methods for precipitation fields using the physically based and spatially distributed model of river runoff on the example of the Gharesou basin, Iran. *Russ. Meteorol. Hydrol.* **2015**, *40*, 480–488. [CrossRef]
20. Zhang, X.; Lu, X.; Wang, X. Comparison of Spatial Interpolation Methods Based on Rain Gauges for Annual Precipitation on the Tibetan Plateau. *Pol. J. Environ. Stud.* **2016**, *25*, 1339–1345. [CrossRef]
21. Foehn, A.; Hernández, J.G.; Schaefli, B.; De Cesare, G. Spatial interpolation of precipitation from multiple rain gauge networks and weather radar data for operational applications in Alpine catchments. *J. Hydrol.* **2018**, *563*, 1092–1110. [CrossRef]

22. Guo, B.; Zhang, J.; Meng, X.; Xu, T.; Song, Y. Long-term spatio-temporal precipitation variations in China with precipitation surface interpolated by ANUSPLIN. *Sci. Rep.* **2020**, *10*, 1–17. [CrossRef] [PubMed]
23. Soleymani Moghadam, M.; Bani Assad, T. An analysis of the urban network of Khorasan Razavi province during the years 1986 to 2011. *Q. J. Geogr. Urban Plan. Zagros Vis.* **2017**, *9*, 45–67. (In Persian)
24. Sakhdari, H.; Ziaei, S. Khorasan Razavi agricultural development priorities: Hierarchical Analysis (AHP) approach. *J. Agric. Econ. Res.* **2018**, *1*, 207–224. (In Persian)
25. Araste, M.; Kaboli, H.; Yazdani, M. Assessing the impacts of meteorological drought on yield of rainfed wheat and barley (Case study: Khorasan Razavi province). *Sci. J. Agric. Meteorol.* **2017**, *5*, 15–25.
26. Emadodin, I.; Reinsch, T.; Taube, F. Drought and desertification in Iran. *Hydrology* **2019**, *6*, 66. [CrossRef]
27. Alijani, B.; Herman, J.R. Synoptic climatology of precipitation in Iran. *Ann. Assoc. Am. Geogr.* **1985**, *75*, 404–416. [CrossRef]
28. Chang, K. *Introduction to Geographic Information Systems*, 3rd ed.; McGrawHill: New York, NY, USA, 2006.
29. Aguilar, F.J.; Agüera, F.; Aguilar, M.A.; Carvajal, F. Effects of precipitation morphology, sampling density, and interpolation methods on grid DEM accuracy. *Photogramm. Eng. Remote Sens.* **2005**, *71*, 805–816. [CrossRef]
30. Xie, Y.; Chen, T.B.; Lei, M.; Yang, J.; Guo, Q.J.; Song, B.; Zhou, X.Y. Spatial distribution of soil heavy metal pollution estimated by different interpolation methods: Accuracy and uncertainty analysis. *Chemosphere* **2011**, *82*, 468–476. [CrossRef] [PubMed]
31. Bhattacharjee, S.; Mitra, P.; Ghosh, S.K. Spatial interpolation to predict missing attributes in GIS using semantic kriging. *IEEE Trans. Geosci. Remote Sens.* **2013**, *52*, 4771–4780. [CrossRef]
32. Wood, C.; Miller, B. *Comparing Simple and Ordinary Kriging Methods for 2015 Iowa Precipitation*; Geological and Atmospheric Sciences; College of Liberal Arts and Sciences, Iowa State University: Ames, IA, USA, 2016.
33. Lichtenstern, A. Kriging Methods in Spatial Statistics. Bachelor's Thesis, Department of Mathematics, Technical University of Munich, Munich, Germany, 2013.
34. İmamoğlu, M.Z.; Sertel, E. Analysis of different interpolation methods for soil moisture mapping using field measurements and remotely sensed data. *Int. J. Environ. Geoinform.* **2016**, *3*, 11–25. [CrossRef]
35. Maris, F.; Kitikidou, K.; Angelidis, P.; Potouridis, S. Kriging interpolation method for estimation of continuous spatial distribution of precipitation in Cyprus. *Curr. J. Appl. Sci. Technol.* **2013**, 1286–1300. [CrossRef]
36. Qing, L.I.; Yu, Y.A.N.G. Cross-Modal Multimedia Information Retrieval. In *Encyclopedia of Database Systems*; Springer: Berlin/Heidelberg, Germany, 2009; pp. 528–532.
37. Sun, Y.; Kang, S.; Li, F.; Zhang, L. Comparison of interpolation methods for depth to groundwater and its temporal and spatial variations in the Minqin oasis of northwest China. *Environ. Model. Softw.* **2009**, *24*, 1163–1170. [CrossRef]
38. Gan, W.; Chen, X.; Cai, X.; Zhang, J.; Feng, L.; Xie, X. Spatial interpolation of precipitation considering geographic and topographic influences—A case study in the Poyang Lake Watershed, China. In Proceedings of the 2010 IEEE International Geoscience and Remote Sensing Symposium, Honolulu, HI, USA, 25–30 July 2010; pp. 3972–3975.
39. Yang, G.; Zhang, J.; Yang, Y.; You, Z. Comparison of interpolation methods for typical meteorological factors based on GIS—A case study in Ji Tai basin, China. In Proceedings of the 19th International Conference on Geoinformatics, Shanghai, China, 24–26 June 2011; pp. 1–5.
40. Wu, C.Y.; Mossa, J.; Mao, L.; Almulla, M. Comparison of different spatial interpolation methods for historical hydrographic data of the lowermost Mississippi River. *Ann. GIS* **2019**, *25*, 133–151. [CrossRef]
41. Magnard, C.; Werner, C.; Wegmüller, U. *GAMMA Technical Report: Interpolation and Resampling*; Gamma Remote Sensing Research and Consulting AG: Bern, Switzerland, 2017.
42. Goovaerts, P. Kriging and semivariogram deconvolution in the presence of irregular geographical units. *Math. Geosci.* **2017**, *40*, 101–128. [CrossRef]
43. Mehrshahi, D.; Khosravi, Y. The assessment of Kriging interpolation methods and Linear Regression based on digital elevation model (DEM) in order to specify the spatial distribution of annual precipitation (Case study: Isfahan Province). *J. Spatial Plan.* **2010**, *14*, 233–249.
44. Mahmoudvand, S.; Khodayari, H.; Tarnian, F. Mapping Bioclimatic Variables Using Geostatistical and Regression Techniques in Lorestan Province. *JGSMA* **2020**, *1*, 1–17. (In Persian)
45. Dirks, K.N.; Hay, J.E.; Stow, C.D.; Harris, D. High-resolution studies of precipitation on Norfolk Island Part II: Interpolation of precipitation data. *J. Hydrol.* **1998**, *208*, 187–193. [CrossRef]
46. Ahrens, B. Distance in spatial interpolation of daily rain gauge data. *Hydrol. Earth Syst. Sci.* **2006**, *10*, 197–208. [CrossRef]
47. Keblouti, M.; Ouerdachi, L.; Boutaghane, H. Spatial interpolation of annual precipitation in Annaba-Algeria—Comparison and evaluation of methods. *Energy Procedia* **2012**, *18*, 468–475. [CrossRef]
48. Martinez, C.A. Multivariate geostatistical analysis of evapotranspiration and precipitation in mountainous terrain. *J. Hydrol.* **1996**, *174*, 19–35. [CrossRef]
49. Goovaerts, P. Geostatistical approaches for incorporating elevation into the spatial interpolation of rainfall. *J. Hydrol.* **2000**, *228*, 113–129. [CrossRef]
50. Wang, X.; Lv, J.; Wei, C.; Xie, D. Modeling spatial pattern of precipitation with GIS and multivariate geostatistical methods in Chongqing tobacco planting region, China. In Proceedings of the International Conference on Computer and Computing Technologies in Agriculture, Nanchang, China, 22–25 October 2010; Springer: Berlin/Heidelberg, Germany, 2010; pp. 512–524.
51. Hu, Y. *Mapping Monthly Precipitation in Sweden by Using GIS*; Göteborg University: Göteborg, Sweden, 2010.

52. Di Piazza, A.; Lo Conti, F.; Noto, L.V.; Viola, F.; La Loggia, G. Comparative analysis of different techniques for spatial interpolation of precipitation data to create a serially complete monthly time series of precipitation for Sicily, Italy. *Int. J. Appl. Earth Obs.* **2011**, *13*, 396–408. [CrossRef]
53. Bostan, P.A.; Heuvelink, G.B.M.; Akyurek, S.Z. Comparison of regression and kriging techniques for mapping the average annual precipitation of Turkey. *Int. J. Appl. Earth Obs.* **2012**, *19*, 115–126. [CrossRef]
54. Hao, W.; Chang, X. Comparison of spatial interpolation methods for precipitation in Ningxia, China. *Int. J. Sci. Res.* **2013**, *2*, 181–184.
55. Abo-Monasar, A.; Al-Zahrani, M.A. Estimation of rainfall distribution for the southwestern region of Saudi Arabia. *Hydrol. Sci. J.* **2014**, *59*, 420–431. [CrossRef]
56. Isaaks, E.H.; Srivastava, R.M. *An Introduction to Applied Geostatistics*; Oxford University Press: New York, NY, USA, 1989.